Ecotoxicology and Environmental Safety 244 (2022) 113980

Contents lists available at ScienceDirect

Ecotoxicology and Environmental Safety

journal homepage: www.elsevier.com/locate/ecoenv

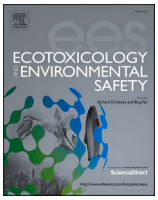

Cell cycle alterations due to perfluoroalkyl substances PFOS, PFOA, PFBS, PFBA and the new PFAS C6O4 on bottlenose dolphin (*Tursiops truncatus*) skin cell

Cristina Otero-Sabio [a], Marta Giacomello [b], Cinzia Centelleghe [a,*], Federico Caicci [b], Marco Bonato [b], Andrea Venerando [a], Jean-Marie Graïc [a], Sandro Mazzariol [a], Livio Finos [c], Livio Corain [d], Antonella Peruffo [a]

[a] Department of Comparative Biomedicine and Food Science, University of Padova, Legnaro, PD, Italy
[b] Department of Biology, University of Padua, Padua, Italy
[c] Department of Developmental Psychology and Socialization, University of Padua, Padua, Italy
[d] Department of Management and Engineering, University of Padova, Vicenza, VI, Italy

ARTICLE INFO

Edited by: Professor Bing Yan

Keywords:
PFAS
Cytotoxicity
Cell line
Tursiops truncatus

ABSTRACT

Per- and polyfluoroalkyl substances (PFAS) have become ubiquitous environmental contaminants in aquatic ecosystems worldwide. Marine mammals, as top predators, are constantly exposed to several PFAS compounds that accumulate in different tissues. As a proxy to assess cytotoxicity of PFAS in the bottlenose dolphin (*Tursiops truncatus*), we generated a new immortalized cell line derived from skin samples of bottlenose dolphin. Using high content imaging, we assessed the effects of increasing concentrations of PFOS, PFOA, PFBS, PFBA and C6O4 on cell viability and cell cycle phases. In particular, we classified all cells based on multiple morphometric differences of the nucleus in three populations, named respectively "Normal" (nuclei in G0, S and M phase); "Large" (nuclei showing characteristics of senescence) and "Small" (nuclei with fragmentation and condensed chromatin). Combining this approach with cell cycle analysis we determined which phases of the cell cycle were influenced by PFAS. The results revealed that the presence of PFOS, PFBS and PFBA could increase the number of cells in G0+G1 phase and decrease the number of those in the S phase. Moreover, PFOS and PFBS lowered the fraction of cells in the M phase. Interestingly PFOS, PFBS and PFBA reduced the prevalence of the senescence phenotype ("large" nuclei), suggesting a potential tumorigenic effect. Besides, the presence of PFOS and PFBS correlated also with a significant decrease in the number of "small" nuclei. The C6O4 exposure did not highlighted morphometric alteration or cell cycle modification bottlenose dolphin skin cell nuclei. While the effects of PFAS on cell cycle was clear, no significant change was detected either in term of cell proliferation or of viability. This study fosters the overall knowledge on the cellular effects of perfluoroalkyl substances in marine mammals.

1. Introduction

PFAS refer to a large family of industrial chemicals that have been produced since the late 1940 s which are highly soluble in aquatic environments. The presence of the carbon-fluorine bonds, makes these compounds extremely stable over time (Shahsavari et al., 2021). The physicochemical properties of PFAS are attributable to their structure and composition: perfluorobutane sulfonate (**PFBS**) and perfluorooctane sulfonate (**PFOS**) are characterized by sulfonic acids as functional group, while perfluorobutanoic acid (**PFBA**) and perfluorooctanoic acid (**PFOA**) carry carboxyl groups. It should be noted that **PFOS** and **PFOA** are long-chain PFAS (C_8) known to be highly persistent, widely distributed, with a high bioaccumulation potential in living organisms and high toxicity for both human and wildlife (Bonato et al., 2020). Research into new and safer alternatives to long-chain PFAS is a rapidly emerging field, which exponentially grow in the last years: the short chain PFAS apparently increase their solubility and in vivo clearance, displaying lower affinity for cell surface receptors in living organisms (Liu et al., 2020). The short-chain perfluoro([5-methoxy-1,3-dioxolan-4-yl]oxy) acetic acid (C6HF9O6, C_4), commercially known as **C6O4**

* Correspondence to: Department of Comparative Biomedicine and Food Science, University of Padova, 16 viale dell'Università, 35020 Legnaro, PD, Italy.
E-mail address: Cinzia.centelleghe@unipd.it (C. Centelleghe).

https://doi.org/10.1016/j.ecoenv.2022.113980
Received 15 January 2022; Received in revised form 12 August 2022; Accepted 13 August 2022
Available online 31 August 2022

or F-Diox acid is a recently introduced chemical as an alternative to long-chain PFASs. The chemical properties of C6O4 make it a highly soluble compound, that completely dissociates in water and is highly biodegradable.

In **mammal species**, the effects of PFAS have been studied in rodent models as mouse and rat. It has been reported that exposure to PFAS affects reproductive performance, contributing to post-natal mortality (Luebker et al., 2005). PFOA toxicity to the endocrine system was reported in mouse, where it leads to early pregnancy loss and to compromised postnatal survival (Lau et al., 2006). Mounting evidence suggests that PFAS can also induce alteration at immune level: DeWitt and colleagues reported that PFOA and PFOS could alter inflammatory responses, production of cytokines, adaptive and innate immune responses in rodent models (DeWitt et al., 2012).

In **human**, numerous studies found significant associations among PFAS exposure and altered immune system response. Data on tumorigenic effects are still a matter of debate, while insufficient data are available to define the impact of PFAS exposure on neurodevelopmental stages (Sunderland et al., 2019).

Marine mammals, as top predators, are exposed constantly to perfluoroalkyl compounds which accumulate in different organs. High levels of PFAS have been found in many species, with interspecific differences due to the different metabolic capacity (Fair and Houde, 2018). Interestingly, a continuous surveillance study from 2002 to 2014 highlighted that the concentration of PFBS gradually increased in cetacean samples, eventually shifting the bioaccumulation pattern from PFOS to PFBS (Lam et al., 2016). PFAS (especially long-chain PFAS, primarily PFOS and PFOA) have been detected in marine mammals tissue (Sturm and Ahrens, 2010). Particularly, high levels of PFOS and PFOA have been reported in **several tissues** of bottlenose dolphin, including the liver (López-Berenguer et al., 2020), plasma (Lynch et al., 2019), blubber (Fair et al., 2010) and muscle (López-Berenguer et al., 2020). Recently, the presence of PFAS have been investigated in **hepatic tissue samples** of 20 bottlenose dolphins stranded along the northern Adriatic Sea coastline between 2008 and 2020: demonstrating that PFOS accounted for up to 71% of all the PFAS profiles (Sciancalepore et al., 2021).

Notably, short-chain PFAS have so far received little or no attention. For instance, no reports of accumulation of C6O4 on marine mammals have been published to date.

Despite the fact that living animals can be exploited to investigate in vivo toxic effects, cell culture models can be used for in vitro studies to reveal specific toxic mechanisms and metabolic processes. The first in vitro evaluation of the ability of PFAS to induce cytotoxicity in mammalian cells line was published twenty years ago.

Over the years, PFOA was shown to induce apoptosis and perturb cell cycle after exposure to 50–150 μM in a dose- and time-dependent manner, with genotoxic effects, causing oxidative DNA damage (Shabalina et al., 1999) in human hepatoblastoma cells. In human hepatocytes cultures, it caused an increase in the expression of genes involved in cell stress responses (Wen et al., 2020), in a dose- and chain length-dependent manner in the rat (Bjork and Wallace, 2009). In a similar manner, it was found that PFOS inhibited intercellular communication in a dose-dependent fashion and promoted differentiation in rat epithelial liver cells and neuronotypic PC12 cells (Hu et al., 2002; Slotkin et al., 2008), while PFBS seemed to counter these effects. In dolphin epidermal and kidney cells, PFOS also inhibited gap junctions and altered gene expression patterns, inducing cell stress responses, blockade of cell cycle progression and cellular proliferation (Mollenhauer et al., 2009). In other human cell lines, PFOA and PFOS have also recently been shown to disrupt endocrine thyroid cells and promote thyroid, breast and lung cancer via epigenetic modifications, proliferation dysregulations and G0/G1 to S phase transition promotion (Coperchini et al., 2017; Pierozan and Karlsson, 2018; Jabeen et al., 2020), whereas C6O4 exposure did not modify significantly cell proliferation (Coperchini et al., 2021).

All these data highlight that cell lines can help to assess the cellular consequences of perfluoroalkyl substances in vitro, likely suggesting in vivo tissue-specific responses. Thus, mammalian cell lines provide a tool for rapid and cost-effective screening of PFAS effects.

Despite the growing number of studies showing that PFAS are frequently found in a wide variety of tissues in marine mammals, the toxic outcomes of PFAS in cetaceans cells remain poorly explored. In the present study we assessed mechanisms and effects of PFAS, namely.

PFOS, PFOA, PFBS, PFBA and C6O4, on a new cell line derived from a skin sample of the bottlenose dolphin, whose population in the Mediterranean Sea has been categorized as "Vulnerable" by the International Union for Conservation of Nature (IUCN) Red List of Threatened Species. Interestingly, our data identify for the first time dose- and compound-specific changes in cell cycle progression.

2. Materials and methods

2.1. Cell line establishment

Primary cell cultures were derived from bottlenose dolphin's skin samples. Tissue samples were collected from dead adult male stranded in January 2019 along the Veneto costline, North Adriatic Sea, (Italy). Primary cell culture was obtained following an established laboratory protocol (Suman et al., 2012), by means of a papain-based dissociation kit (Worthington Biochemical Corporation, Lakewood, NJ, USA). Cells were then suspended in a medium for cell culture consisting of a 1:1 mixture of DMEM and Ham's F-12 (Biowest®), supplemented with penicillin (30 mg l^{-1}), streptomycin (50 mg l^{-1}) (Pan Biotech™) and 10% fetal bovine serum (FBS Good, Pan Biotech™). Cells were maintained in an incubator under standard conditions at 37 °C with 5% CO_2 and humidified atmosphere. Cell culture medium was replaced with fresh media 24 h after and every 2–3 days until cells reached 80% confluence.

To obtain a stable cell line, primary cell cultures were transfected with pSV3neo plasmid (LGC Promochem, Teddington, UK) using GenJet™ In Vitro DNA Transfection Reagent (Ver. II, SignaGen® Laboratories) following the manufacturer instructions.

To validate the cetacean species as well as cells immortalization, short tandem repeat (STR) genetic profile analysis and polymerase chain reaction (PCR) analysis have been performed by the Leibniz Institute DSMZ-German Collection of Microorganisms and Cell Cultures GmbH, Germany. This cell line belongs to the patent Sea Sentinels System (S.S.S.), (patent n° 102020000003248; https://www.knowledge-share.eu/en/patent/sea-sentinel-system-for-environmental-studies/).

2.2. Cell cryopreservation and thawing

Immortalized cells were cryopreserved at − 80 ºC in a cryopreservation medium consisting of a mixture of 90% (v/v) FBS and 10% (v/v) dimethyl sulfoxide (DMSO).

2.3. Cell line characterization by immunocytochemical analysis

Immunocytochemical analyses were performed to characterize the immortalized cell line. After fixation with 4% paraformaldehyde (PFA) in PBS, cells were gently washed with PBS 1X, permeabilized with 0.1% Triton X-100 for 10 min at 4 °C, treated with 5% BSA in PBS 1X for 30 min and then incubated overnight with the following primary antibodies: anti-vimentin 1:200 (GeneTex Inc, Clone GT7812, Cat# GT7812), anti-cytokeratin 1:50 (Dako, Clone AE1/AE3, Cat# M3515), anti-β-actin 1:500, (hereafter actin, Sigma-Aldrich, Clone AC-74, Cat# A2228). Cells were then incubated for 1 h with the anti-mouse Alexa Fluor® 488 IgG at a dilution 1:400 (Biotium, Cat# A32733). Nuclei were stained with Hoechst 33342 (Sigma-Aldrich). Finally, the labeled cultures were observed under a Leica TCS SP5 confocal microscope.

2.4. Transmission electron microscopy observation (TEM)

Immortalized cells were seeded in 6-wells plates. At confluence, cells were fixed with 2.5% glutaraldehyde in 0.1 M sodium cacodylate buffer (pH 7.4) at 4 °C. Samples were post-fixed with a mixture containing 1% osmium tetroxide and 1% potassium ferrocyanide in a 0.1 M sodium cacodylate buffer for 1 h at 4° C. After three washes with water, samples were dehydrated by immersion in increasing concentrations of ethanol and embedded in epoxy resin (Sigma-Aldrich). Ultrathin sections (60–70 nm) were obtained with an Ultrotome V (LKB) ultramicrotome, counterstained with uranyl acetate and lead citrate. Samples were observed with a Tecnai G 2 (FEI) TEM operating at 100 kV and images were acquired with a Veleta digital camera (Olympus Soft Imaging System).

2.5. Experimental design, chemical preparations and working solutions analysis

The PFAS stock solutions (20 mM) were prepared from PFOS (CAS no. 1763–23–1), PFOA (CAS no. 335–67–1), PFBS (CAS no. 375–73–5), PFBA (CAS no. 375–22–4), and the C6O4 (Wellington Laboratories Inc, CAS no. 1190931–41–9); either by mixing liquid chemical or dissolving neat chemical in to DMSO (>99:9%), aliquots were stored at − 80 °C.

The working solutions containing the PFAS at the different concentrations tested were prepared by the stock solution aliquots and performing serial dilutions in DMSO and DMEM. Before exposing the cells to the diverse experimental conditions of PFOS, PFOA, PFBS, PFBA and C6O4, we determined the concentrations of PFAS, in the working solutions.

The measured concentrations of PFOS, PFOA, PFBS, PFBA and C6O4 were analyzed with high-performance liquid chromatography (HPLC) system and triple quadrupole mass spectrometer, at the laboratory Merieux NutriSciences Italia, Rag. Soc. Chelab S.r.l. Results are reported in Table 1. The concentrations were determined by internal standard technique using isotopically labeled internal standards and calibration standards prepared in solvent.

Cells were seeded at a density of 10,000 cells/well in a 96-well ViewPlate-96 F TC (PerkinElmer®). All PFAS analyzed were tested in parallel in the 96-well plate. For each experiment, 250 μl/well of working solution was used. Four independent experiments were performed, each with three replicates per condition.

Table 1
Mean values of PFOS, PFOA, PFBS, PFBA and C6O4 concentration (measured concentration), analyzed in the working solutions.

Compound	Expected concentration (μM)	Measured concentration (μM)
PFOS	100	85.4 ± 2.5
	10	8.51 ± 0.29
	1	0.87 ± 0.04
	0,1	0.084 ± 0.003
	0,01	0.0087 ± 0.0004
PFOA	100	93.9 ± 1.02
	10	9.1 ± 0.44
	1	0.89 ± 0.03
	0,1	0.085 ± 0.001
	0,01	0.0080 ± 0.0005
PFBS	100	90.7 ± 1.88
	10	9.21 ± 0.35
	1	0.92 ± 0.03
	0,1	0.087 ± 0.007
	0,01	0.0080 ± 0.0005
PFBA	100	89.1 ± 2.9
	10	8.5 ± 0.26
	1	0.87 ± 0.02
	0,1	0.085 ± 0.006
	0,01	0.0086 ± 0.0003
C_6O_4	1	0.91 ± 0.02
	0,1	0.09 ± 0.002
	0,01	0.0087 ± 0.0004

Cells were than incubated at 37 ºC and 5% CO2 for 48 h. After exposure to PFAS, cells were fixed with 1% PFA and stained with Hoechst for 30 min at room temperature.

Brightfield and Hoechst 33342 fluorescence images were acquired using a 20X long WD objective in the High Content Screening imaging system Operetta® (PerkinElmer, Monza, Italy). Analysis was performed using the Harmony software (PerkinElmer).

2.6. Nuclear morphometric-parameters definition and nuclei classification

The morphological domains considered (Intensity, Size and Regularity) and the description of the morphometric parameters measured in the cells nuclei are summarized in Table 2.

The morphometric parameters values have been obtained upon fully automated image analysis (software Harmony, PerkinElmer®).

2.7. Nuclear classification

Data analysis approach was set up by combining the size parameter (nuclear length), the nuclei regularity (Inv/AR) and the nuclear Hoechst intensity (Nuclear intensity). This procedure allowed us to classify each individual cell nucleus in three populations and eight groups, named respectively Normal nuclei population (divided in to four groups); Large nuclei population (divided in to two groups) and Small nuclei population (divided in to two groups). Cell nuclei resulted classified into three populations, respectively named as follows: Normal population (divided in four groups depending on the cell cycle phase); Large population (divided in two groups) showing characteristics of senescence, and Small population (divided in two groups) showing typical apoptosis features (Table 3).

2.8. Cell proliferation assay

To analyze the cell vitality, the cell nuclei number was counted in each experimental condition (PFAS and concentration tested), and compared to the control (1% DMSO). To describe the dose response effect to different PFASs we considered the average number of cell nuclei per condition.

Table 2
Morphological domains, nuclear morphometric parameters and parameters description.

Morphological domains	Morphometric parameter	Description/mathematical formula
Intensity	Hoechst fluorescence intensity (Intensity)	The intensity values are directly related to chromatin compactness. The higher the value of the intensity, the greater the probability that the analyzed nucleus belongs to a dead cell
Size	Nuclear area (Area)	The nuclear area values are inversely related to chromatin compactness. Cells under apoptosis are characterized by chromatin condensation and a smaller nucleus.
	Nuclear width (Width)	This parameter measure width of the nucleus
	Nuclear length (Length)	This parameter measure the length of the nucleus
Regularity	Ratio 1/(nuclear length/nuclear width), (InvAR)	The value of this parameter ranges from 0 to 1. Values close to 1 indicate regular nucleus shape. Small values of InvAr indicate irregular shape.

Table 3
Classification of the cell nuclei (the three populations were divided in eight groups, each characterized by different nuclear/DNA morphology) based on the matrix plot (Fig. 3).

GROUPS	NUCLEI POPULATIONS	NUCLEAR SHAPE	BIOLOGICAL MEANING	LENGHT REANGE	INTENSITY REANGE	REGULARITY RANGE
1. NORMAL REGULAR NUCLEUS	NORMAL POPULATION	Regular shape and size, weakly stained	Healthy cells (G0)	10–28 μm	2000–7000	0.6 – 0.9
2. NORMAL REGULAR NUCLEUS		Regular shape, intensely stained	DNA Synthesis (S)	10–28 μm	7000–12000	0.6 – 0.9
3. NORMAL IRREGULAR NUCLEUS		Regular shape, strongly stained	G2 + Early mitotic phases (M)	10–28 μm	12000–16000	0.6 – 0.9
4. NORMAL IRREGULAR NUCLEUS		Irregular shape, strongly stained	Mitotic phases (M)	10–28 μm	12000–16000	0.3 – 0.6
5. LARGE REGULAR NUCLEUS	LARGE POPULATION	Regular shape, weakly stained	Cellular senescence, chromatin fading	≥ 28 μm	2000–6000	0.6 – 0.9
6. LARGE IRREGULAR NUCLEUS		Irregular shape, weakly stained	Mitotic catastrophe or nuclear damages events	≥ 28 μm	2000–6000	0.3 – 0.6
7. SMALL REGULAR NUCLEUS	SMALL POPULATION	Regular shape,	Nuclear fragmentation, condensed chromatin	≤ 10 μm	2000–16000	0.6 – 0.9
8. SMALL IRREGULAR NUCLEUS		Irregular shape	Nuclear fragmentation, condensed chromatin	≤ 10 μm	2000–16000	0.3 – 0.6

2.9. MTT cell viability assay

Cell viability after exposure to PFASs compounds was determined by using the 3-(4,5-dimethylthiazol-2-yl)− 2,5-diphenyltetrazolium bromide (MTT) assay after 48 of treatment. Briefly, cells were seeded in 96-wells plates at a concentration of 10,000 cells/ml, and exposed to PFASs at different concentrations (Table 1). After 48 h cells were incubated for 1 h at 37 °C with the MTT solution and absorbance was measured with the multilabel plate reader VICTOR™ X4 (PerkinElmer®). Three individual experiments were performed, each with 4 replicates per condition. As a readout for cell viability, we calculated the ratio between the absorbance of treated cells/absorbance of control cells* 100 (%). EC_{50} values were estimated from dose–response curves.

2.10. Cell cycle profiling by Hoechst intensity analysis

Assessment of nuclear Hoechst intensity was carried out by automated image analysis (Harmony software, PerkinElmer®). Cell

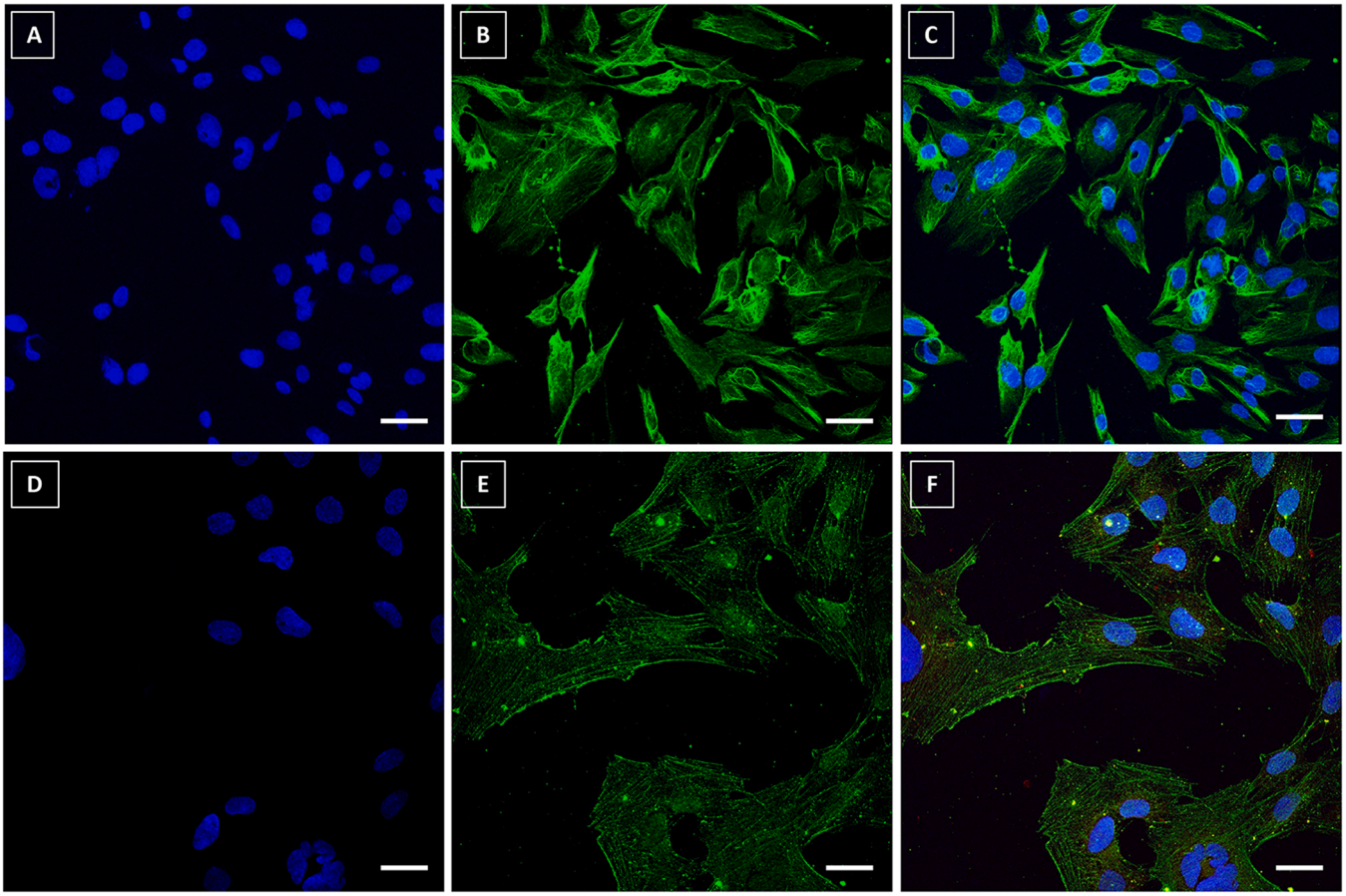

Fig. 1. Confocal images of immunocytochemical detection of the vimentin antibodies in the *Tursiops truncatus* skin cell line. In A Hoechst-staining image of the cell nuclei, in B vimenti-ir cells, in C superimposed confocal images of A and B images (scale bar 20 μm). In D Hoechst-staining image of the cell nuclei, in E actin-ir cells, in F merge of D and E image (scale bar 40 μm).

aggregates were gated out of the analysis. We plotted the frequency of cell nuclei within fixed Hoechst intensity ranges (2000–6000, 6000–12000 and 12000–16000). Based on Hoechst staining, cells were assigned to G0, S, and M phases. Cell cycle phases G0 +G1, S, and G2 +M, were defined by applying manual gates to the cell cycle histogram (Roukos et al., 2015; Schorpp et al., 2016).

2.11. Statistical methodology

The statistical analysis compared the control condition to each experimental condition tested. Our approach took into account the distribution of the nuclei based on the combination of the above mentioned parameters. After classification of cells in different groups according to their nuclear features, a series of nonparametric rotation tests (Solari et al., 2014) was performed, allowing comparison of each experimental condition versus control. The analysis performed was equivalent to a nonparametric one-to-many repeated measures ANOVA, where the repetitions are among plate and group. The statistical significance was defined by mean of a nonparametric Fisher test (Pesarin, 2001). The analysis has been performed with R software (R Core Team, 2021) and *flip* package (Finos, 2018).

3. Results

3.1. Tursiops truncatus skin cell line characterization

Ultrastructure of the *Tursiops truncatus* skin cell line characterized by immunofluorescence targeting vimentin and actin are showed in (Fig. 1). The cell line revealed immunoreactivity (-ir) for vimentin, a cytoskeletal protein typically expressed in mesenchymal cells. The vimentin-ir cells showed cytoplasmic filamentous structures, consistent with the presence of intermediate filaments typical of fibroblast cells. Immunodetection of actin-ir cells allowed us to further define the cytoarchitecture of this new cell model.

3.2. Cells ultrastructure analysis by TEM

We used TEM analysis to reveal ultrastructural details. Generally, all analyzed cells exhibited polymorphic nuclei, with predominance of euchromatin (Fig. 2A, C, D, E), indicating active transcription. In the cytoplasm, mainly alongside the nucleus, well-developed cisternae of endoplasmic reticulum were visible, moreover, numerous mitochondria and polyribosome were present, characteristic of cells with intense protein synthesis (Fig. 2 B, C, E, F). A few intracytoplasmic lamellar bodies and autophagic bodies were also present in the cytosol (Fig. 2 B, C, F).

3.3. Cell proliferation and viability assays did not show difference after PFAS treatment

The cell proliferation assay did not show significant changes of the cell nuclei density at any PFOS, PFOA, PFBS, PFBA and C6O4 condition tested, compared to the control (Fig. 3A).

The cell viability analysis performed by MTT Assay did not show significant difference in cell viability at any PFAS condition tested. Details are reported in the supplementary material (Fig. S1).

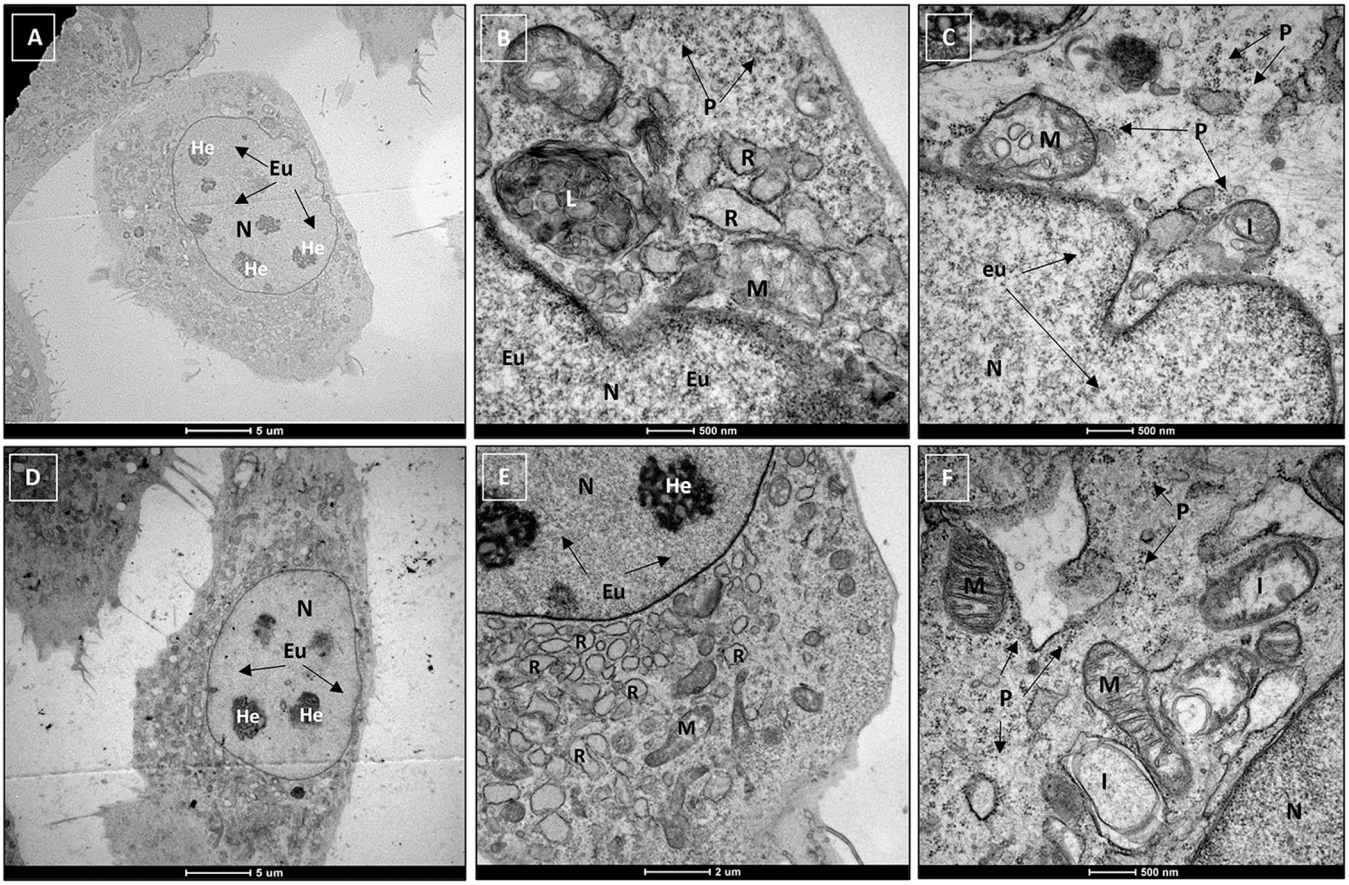

Fig. 2. Details of TEM images of the cells derived from *Tursiops truncatus* skin. In A and D and E images, details of cells showing irregular shaped nuclei (N), containing heterochromatin (He) and mainly euchromatin (Eu). In B, E and images, in the cytoplasm alongside the nucleus, are well-developed cisternae of rough endoplasmic reticulum (R), forming vesicles, or greatly enlarged. Mitochondria (M) and polyribosome (P) were present in the cytosol as shown in the image B, C and F). A few intracytoplasmic multi-lamellar bodies (I) and autophagic bodies (CF) were also present in the cytosol as shown in the image B, C, F.

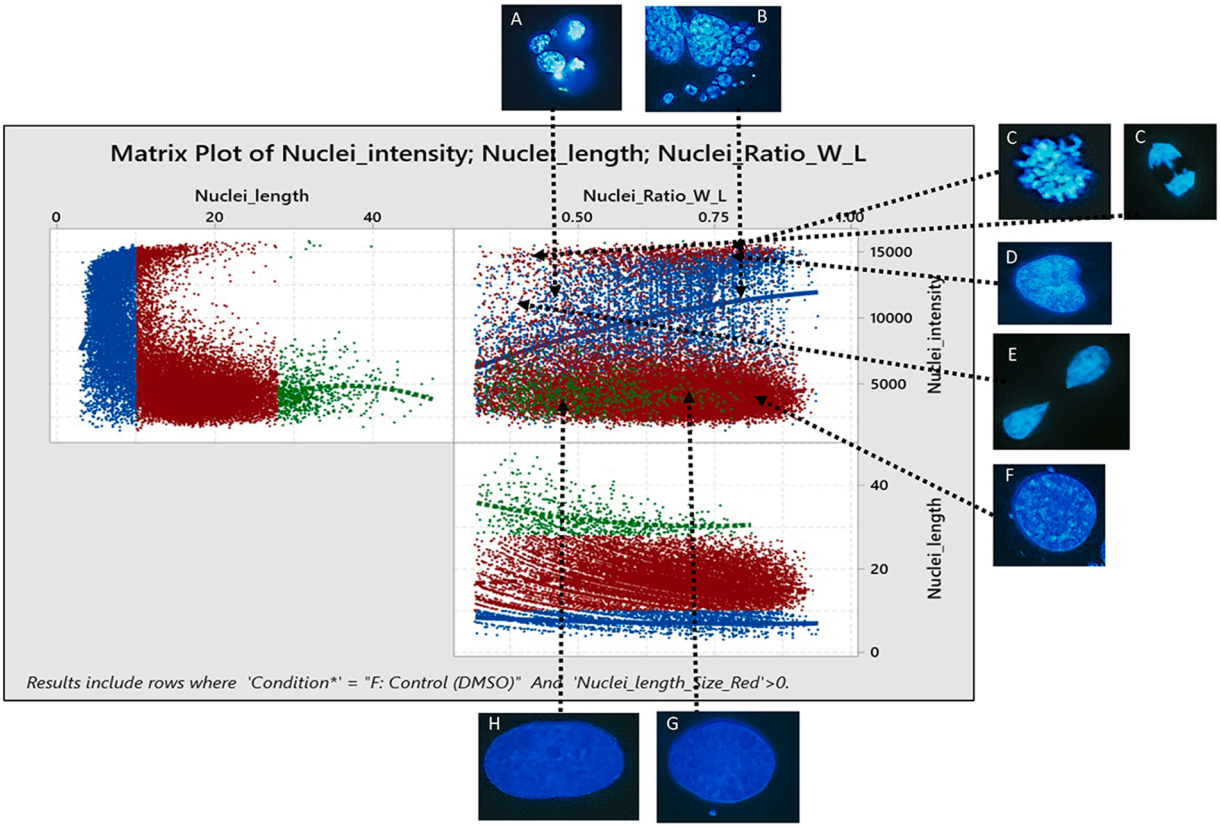

Fig. 3. Matrix plot distribution of the nuclei based on the parameters "nuclei length" versus "nuclei intensity" versus "nuclei Ratio W-L (InvAR)" in the control condition: the red dots represent the normal nuclei groups; the green dots represent **the** large nuclei groups; the blue dots represent the small nuclei. Image A, example of a small irregular nucleus. Image B, example of a small regular nucleus. Image C, example of a normal nucleus in mitotic phase. Image D, example of a normal nucleus in DNA-Synthesis phase. Image E, example of a normal nucleus at the end of the mitosis phase. Image F, example of a normal nucleus in G0 +G1 phase. Image G, example of a large nucleus with low Hoechst intensity and regular shape. Image H, example of a large nucleus with low Hoechst intensity and irregular shape (Hoechst images were acquired at the Leica TCS SP5 confocal microscope.

3.4. Nuclear classification results

The results of the combinations of the selected morphometric parameters (nuclei length versus nuclei intensity versus InvAR) were plotted: the resulting cell nuclei distribution in the control condition is represented in the matrix plot (Fig. 3).

3.5. Generation of cell cycle profiles in the Normal, Large and Small nuclei population after PFAS treatment

We calculated and plotted the frequency distributions of the integrated Hoechst intensity of cell nuclei per each experimental condition tested, and we generated the cell cycle profiles by gating nuclei within the different cell cycle phases. The profile of the cell nuclei and the respective frequency distributions in G0 + G1 phase, S phase and G2 + M phase were determined per each experimental condition and plotted into histograms. As an example, we show the results after treatment with 1 μM PFBA, PFBS, PFOA, PFOS and C6O4, per each population (Fig. 4). Results for the other concentrations used are reported in the supplementary material (Figs. S2-S5).

In the Normal population our analysis allowed to clearly differentiate cells in G0 +G1 phase, S phase and G2 +M phase (Fig. 4), showing a distribution that indicates the common chromosome segregation and duplication found in cells with high genome stability.

The Large and the Small nuclei populations exhibited derangements of the cell cycle profile and the progression of the cell cycle did not match whit that of the Normal population.

3.6. Dose response effects: PFOS, PFBS and PFBA induce dysregulation in the cell cycle

To determine how PFAS affected either the distribution of nuclei in the different population (Normal, Large or Small) or their cell cycle phase, the respective nuclei count after PFOS, PFBS, PFBA, PFOA and C6O4 exposure have been analyzed and compared to the control condition.

The results revealed that PFOS, PFBS and PFBA alter the cell cycle ($p < 0.05$). Conversely, no significant effect was detected for PFOA and C6O4 at any concertation tested, see supplementary material (Table S1).

In detail, exposure to **PFOS** at the lower concentrations (0.01 μM and 0,1 μM) did not show significant effects while higher concentrations 1 μM, ($p = 0.026$); 10 μM, ($p = 0.040$) and 100 μM ($p = 0.018$) increased the number of nuclei belonging to the population in the G0 +G1 cell cycle phase (group 1) and decreased the amount in the S phase, 1 μM, ($p = 0.033$); 10 μM, ($p = 0.010$) and 100 μM ($p = 0.041$), (Table 3). Moreover, 1 μM PFOS significantly lowered the number ($p = 0.037$) of nuclei in the M phase and the amount of cell nuclei in the Large population likely in the senescence phase ($p = 0.05$ and $p = 0.037$), (group 5 and 6), (Table 3). Interestingly, 1 μM PFOS decreased nuclei in the Small population ($p = 0.045$), characterized by fragmentation and condensed chromatin (group 8), (Table 3).

Exposure to **PFBS** at 0.01 μM did not show significant effects; while higher concentrations 0.1 μM, ($p = 0.032$); 1 μM ($p = 0.006$), 10 μM ($p = 0.019$) and 100 μM ($p = 0.019$) caused a significant increase of nuclei in the Normal population in the G0 +G1 cell cycle phase. At 0.01 μM, ($p = 0.011$); 0.1 μM, ($p = 0.038$); 1 μM, ($p = 0.010$); and

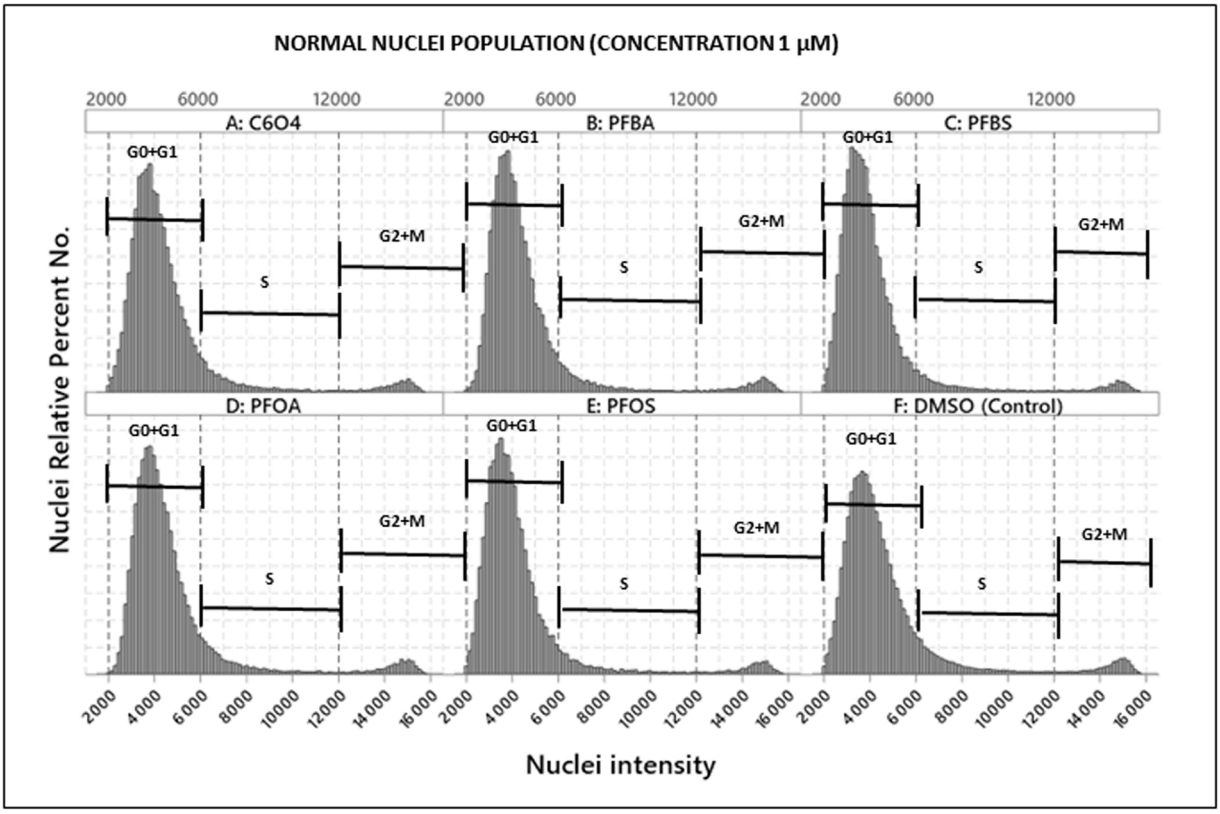

Fig. 4. Histogram of the cell cycle profile for the Normal nuclei population of the *Tursiops truncatus* skin-derived cells for the following treatment: 1 µM C6O4, PFBA, PFBS, PFOA, PFOS. In each histogram is shown the relative cells percentage (Y axis) in relation to the intensity (X axis). Normal nuclei population displaying the G0 +G1 cells (representing 2 n DNA content), S (DNA synthesis) and G2 +M diploids cells (representing 4 n DNA content) in the control condition (histogram F) and after cells exposure to PFA. The percentage of cells in a specific phase has been determined by means of Hoechst intensity. Mitosis cells (4 n DNA content) have a doubled intensity when compared to G1 cells (2 n DNA content).

100 µM, ($p = 0.025$), PFBS, we observed a decreased number of nuclei in the S phase (Table 3). PFBS at a concentration of 0.1 µM and 1 µM altered the number of nuclei in the M phases (group 3 and 4) and showed a significant decrease ($p = 0.050$ and $p = 0.036$ respectively) in the large population nuclei (group 6), (Table 3). In addition, 1 µM PFBS significantly decreased ($p = 0.042$) the number of nuclei in the Small population (group 8), (Table 4).

Exposure to **PFBA** at 0.01 µM, ($p = 0.024$); 0,1 µM, ($p = 0.008$) and 1 µM, ($p = 0.017$); significantly increased the cell nuclei number in the Normal population, specifically in the G0 +GT1 phase (group 1). At 0.1 µM, it increased ($p = 0.020$) the number of nuclei in the M phases (group 4) while at 1 µM, PFBA decreased ($p = 0.054$) the number of nuclei in the S phases (group 2). At the concentrations of 0.01 µM, ($p = 0.020$); 0.1 µM, ($p = 0.070$); 1 µM, ($p = 0.042$) PFBA significantly decreased the number of nuclei in the Large population (group 5 and 6), (Table 3).

Table 4
Results of the inferential analysis for the compound PFOS, PFBS and PFBA combined by groups. Significant p-value ≤ 5%. Arrow (↑) significant increasing in nuclei count, arrow (↓) significant decreasing in nuclei count, (-) no significant. See the corresponding cell cycle histograms at the different experimental conditions of the PFAS tested in comparison to the control condition showing the relative cells percentage (Figs. S2, S3, S4 and S5 in the section Supplementary Material).

	Concentration 0,01 µM	Concentration 0,1 µM	Concentration 1 µM	Concentration 10 µM	Concentration 100 µM
Group 1 G0 + G1 phase	**PFBA** p = 0.024 ↑	**PFBS** p = 0.032 ↑ **PFBA** p = 0.008 ↑	**PFOS** p = 0.026 ↑ **PFBS** p = 0.006 ↑ **PFBA p = 0.017** ↑	**PFOS** p = 0.040 ↑ **PFBS** p = 0.019 ↑	**PFOS** p = 0.018 ↑ **PFBS** p = 0.019 ↑
Group 2 S phase	–	**PFBS** p = 0.011 ↓	**PFOS** p = 0.033 ↓ **PFBS** p = 0.038 ↓ **PFBA p = 0.054** ↓	**PFOS** p = 0.010 ↓	**PFOS** p = 0.041↓ **PFBS** p = 0.025 ↓
Group 3 G2 + Early M phase	–	**PFBS** p = 0.057 ↓	**PFOS** p = 0.037 ↓ **PFBS** p = 0.023 ↓	–	–
Group 4 M phase	–	**PFBS** p = 0.051 ↑ **PFBA** p = 0.020 ↑	**PFBS p = 0.022**↑	–	–
Group 5 Large regular	–	**PFBA** p = 0.014 ↓	**PFBA** p = 0.020 ↓	**PFOS** p = 0.050 ↓	–
Group 6 Large irregular	**PFBA** p = 0.020 ↓	**PFBA** p = 0.070↓	**PFOS** p = 0.037 ↓ **PFBS** p = 0.050 ↓ **PFBA** p = 0.042 ↓	**PFBS** p = 0.036 ↓	–
Group 7 Small regular	–	–	–	–	–
Group 8 Small irregular	–	–	**PFOS** p = 0.045 ↓ **PFBS p = 0.042**↓	–	–

4. Discussion

Due to the impossibility to investigate in vivo in marine mammals the toxic effects of PFAS, we established an in vitro model, which consist of a cell line derived from a skin sample of bottlenose dolphin. In this new model, we analyzed the effects of PFOS, PFOA, PFBS, PFBA and C6O4. We choose a large range of concentrations (from 0.01 to 100 μM) to provide an overview of the effects either at low and high levels of PFAS, and to compare our datasets with those already published (Coperchini et al., 2017; Jabeen et al., 2020).

We found that PFOS and PFBS exposure on *Tursiops truncatus* skin-derived cells increased the number of nuclei in the G0 +G1 phase and decreased the number in S phase. Moreover, PFOS and PFBS induced a significant decrease of nuclei in the G2 +M phases. At variance, PFBA treatment displays an effect only at lower doses. This evidence suggests the possibility that PFBA-induced changes in the cell physiology is a dynamic process, characterized by a hormetic dose-response phenomenon (Calabrese, 2005). Hormesis is a well-known, cell-type specific, phenomenon in the field of toxicology and has been described in different cell lines and dose-response curves of several compounds, especially cancer-related drugs (Bernardini et al., 2021; Günes-Bayir et al., 2020). Evidence of PFAS-associated hormetic response has been highlighted by Reistad and colleagues, who showed that cell death was induced on neurons from rat cerebellum at relatively low concentrations by PFOA (at 25 μM), while higher concentrations lowered the number of dead cells (at 100 μM), (Reistad et al., 2013).

In our study, no significant changes in cell cycle were observed after treatment with C6O4 and PFOA.

Interestingly, the effects of the PFAS used in this study were specific to the cell cycle, without effecting the overall cell proliferation and viability. This outcome underlines the need to study PFAS effects in marine mammals not only in terms of cell viability, but also by considering subcellular pathways that are key for the single cell physiology in primis, and secondly for health and metabolism of the whole tissue and organism.

4.1. Cell nuclei classification and cell cycle profiling

It is known that during the life of cells, changes of nuclear morphology occur normally in mitosis or in processes related to cell death (as nuclear fragmentation observed in apoptosis) or in senescence (Narita et al., 2003).

Monitoring nuclear morphometric parameters may help to reveal alterations of cell cycle. Indeed, nuclear irregularities have already been proposed as a tool to provide a screening of normal, senescent and apoptotic cells (Filippi-Chiela et al., 2012). In fact, nuclear condensation can be used to distinguish apoptotic cells from healthy or necrotic cells (Crowley et al., 2016; Roukos et al., 2015).

Methods to accurately determine and track the cell cycle phases of individual cells and to combine this information with other cellular features assessed by imaging, such as localization of a protein or morphological changes of organelles (Roukos et al., 2015), have been recently developed. These approaches show as chromatin undergoes dramatic condensation and decondensation in the transition between different phases of the cell cycle or of the cell life (Estandarte et al., 2016). Vakifahmetoglu and coworkers (2008) demonstrated that chromatin modifications include nuclear condensation and fragmentation in apoptosis, increased nuclear size during senescence and rise of nuclear irregularity in several conditions, such as chemical stresses, defective activation or inactivation of cell cycle checkpoint processes or exogenous agents that affect chromatin remodeling (Vakifahmetoglu et al., 2008). Considering these studies, our approach based on the combination of three main morphometric parameters (length, intensity and InvAR) to classify the nuclei in three populations (Normal, Large, Small), clearly differentiate the cells in G0 +G2 phase, S phase and G2 +M phase, analyzing the relative distribution of the cell nuclei in each profile (Fig. 4).

4.2. PFOS, PFBS and PFBA alter cell cycle phases despite no effects on cell proliferation and viability

Our study for the first time provides evidence that PFOS, PFBS and PFBA induce dysregulation in the cell cycle of *Tursiops truncatus* living skin cells, as detailed in the results section. Indeed, although few previous data regarding the in vitro effects of PFOS, PFOA, PFBS, PFBA and C6O4 exposure are available, a systemic comparative analysis of their cellular effects in the same model has not been previously described. Scattered results have been reported on in vitro models derived from terrestrial mammals (human and rodents cell lines) and marine mammals cell lines (bottlenose dolphin).

In **terrestrial mammalian species,** some studies investigated the possibility that PFOA and PFOS alter the cell proliferation rate (Coperchini et al., 2017; Jabeen et al., 2020), while the effects of C6O4 and PFBS were assessed in different in vivo and in vitro models (Coperchini et al., 2021). In particular, Coperchini and colleagues used two different lines (**human and rat thyroid cells)** and treated them for 6 days with the same concentrations of C6O4, PFOA and PFOS that we tested in our study (Coperchini et al., 2021). Their results demonstrated that PFOS exposure reduced cell viability in both human and rat cell lines, while PFOA only in rat thyroid cells. PFOS showed the same behavior at all concentrations in the two cell lines, causing a reduction in cell proliferation; instead C6O4 did not affect the proliferation rate of either cell line. Jabeen and colleagues instead studied the effects of PFOA and PFOS on **human lung cell line,** and noticed an increase in proliferation at 100/200 μM of PFOA and PFOS after 24 and 48 h treatment (Jabeen et al., 2020). Shabalina and colleagues (1999) demonstrated that PFOA treatment of **human hepatoblastoma cells** perturbs cell cycle and induces apoptosis after exposure to 50–150 Mm for 48 h. Specifically, 50 μM treatment resulted in a significant increase in the proportion of cells in the M phase and simultaneously a decrease in the number of cells in the S phase, whereas treatment with 100 or 150 μM PFOA increased the proportion of cells in the G0 +G1 phase and decreased the number of cells in the M and S phases (Shabalina et al., 1999). In a study performed on **human breast cells** exposed to 1 and 10 μM PFOS it was demonstrated that the cell growth was higher as compared to the control (Pierozan and Karlsson, 2018).

On the **marine mammalian species**, only few studies have been performed on in vitro models: Hu and colleagues, on a **dolphin kidney epithelial cell line**, showed that PFOS inhibits intercellular communication, while PFBS did not have significant effects within the ranges of concentration tested (Hu et al., 2002); an in vitro study using **skin cell culture from bottlenose dolphin** exposed to PFOS, performed by Mollenhauer and colleagues, reported that PFOS exposure significantly alter normal gene expression patterns, decreasing those involved in cell cycle progression and proliferation (Mollenhauer et al., 2009).

These studies provide evidence that several PFAS tare capable of altering cell proliferation, with differences attributable to the different origin of the cell lines, to the concentrations tested, exposure times. An additional source of variability might be due to the type of test used to evaluate cell viability.

We here provide a comparative and comprehensive study of the effects of five PFAS, highly detected in both terrestrial and marine environments. In particular, the present study shows that PFOS, PFBS and PFBA dysregulate cell proliferation in a bottlenose dolphin skin cell line. Our results are in agreement with several studies that, although in a fragmented fashion, have previously evidenced that PFAS are able of altering cell cycle in different mammals' cell models. At the moment, the molecular mechanisms at the basis of these effects still lack and necessitate further studies, such as advanced data analysis strategies and complex multivariate analyses (Montelli et al., 2017).

However, we must emphasize that a possible interpretation of the results should depend not only on to classific classification of PFAS (long

versus short-chain); but also on the specific properties attributable to the chemistry of their specific functional groups. Indeed, it is worth noting that PFOS and PFBS present fluorinated carbon chains attached to sulfonic acids. Instead, PFBA consists of a fluorinated carbon chains attached to carboxylic acids. The nature of the functional group could be co-responsible in inducing dysregulation in the cell proliferation cycle, thus explaining different results between PFBS and PFOS (that showed their effects at the higher concentrations tested) and PFBA (that resulted significant at the lower concentrations). A first hints on this point of view derives from the study of Hagenaars and colleagues that demonstrated how compounds with the same chain length but different functional groups display different toxic potential. In fact, PFAS with a sulfonate group (as PFBS and PFOS) seem to have a larger toxic potential than those with a carboxyl group (PFBA), (Hagenaars et al., 2011).

5. Conclusion

The main goal of this investigation was to find out and compare cytotoxic effects of PFOS, PFBS and PFBA on bottlenose dolphin skin-derived cells.

Despite the growing number of studies showing as PFAS are frequently found in a wide variety of tissues in marine mammals, the cellular nature of PFAS toxic effects in cetaceans remains poorly understood.

We concluded that exposure to either PFOS, PFOA, PFBS, PFBA or C6O4 did not alter cell viability in the *Tursiops truncatus* skin cells line at the proposed concentrations.

Here, we show that quantifying cell viability alone is insufficient to distinguish between the compound responses. By means of an unbiased high throughput approach to analyze PFAS dose-response effects, we found that compounds with similar cell viability outcomes have different effects on the cell growth.

Funding information

The financial support of this study was approved by the "Proof of Concept (PoC) grant" (CUP C96I20000120004) from the University of Padova and from the Italian Ministry of Economic Development.

CRediT authorship contribution statement

Cristina Otero-Sabio: Methodology, Writing – original draft, Writing – review & editing. **Marta Giacomello**: Methodology, Writing – review & editing. **Cinzia Centelleghe**: Methodology, Writing – review & editing. **Federico Caicci:** Methodology, Writing – review & editing. **Marco Bonato:** Writing – review & editing. **Andrea Venerando:** Methodology, Writing – review & editing. **Jean-Marie Graïc:** Writing – review & editing. **Sandro Mazzariol:** Writing – review & editing. **Livio Finos:** Methodology, Writing – review & editing. **Livio Corain:** Methodology, Writing – review & editing. **Antonella Peruffo**: Conceptualization, Supervision, Writing – original draft, Writing – review & editing.

Declaration of Competing Interest

The authors declare that they have no known competing financial interests or personal relationships that could have appeared to influence the work reported in this paper.

Data availability

No data was used for the research described in the article.

Appendix A. Supporting information

Supplementary data associated with this article can be found in the online version at doi:10.1016/j.ecoenv.2022.113980.

References

Bernardini, I., Matozzo, V., Valsecchi, S., Peruzza, L., Rovere, G.D., Polesello, S., Iori, S., Marin, M.G., Fabrello, J., Ciscato, M., Masiero, L., Bonato, M., Santovito, G., Boffo, L., Bargelloni, L., Milan, M., Patarnello, T., 2021. The new PFAS C6O4 and its effects on marine invertebrates: First evidence of transcriptional and microbiota changes in the Manila clam Ruditapes philippinarum. Environ. Int. 152, 106484 https://doi.org/10.1016/j.envint.2021.106484.

Bjork, J.A., Wallace, K.B., 2009. Structure-activity relationships and human relevance for perfluoroalkyl acid–induced transcriptional activation of peroxisome proliferation in liver cell cultures. Toxicol. Sci. 111, 89–99. https://doi.org/10.1093/toxsci/kfp093.

Bonato, M., Corrà, F., Bellio, M., Guidolin, L., Tallandini, L., Irato, P., Santovito, G., 2020. PFAS environmental pollution and antioxidant responses: an overview of the impact on human field. Int. J. Environ. Res. Public Health 17 (21), 8020. https://doi.org/10.3390/ijerph17218020.

Calabrese, E.J., 2005. Cancer biology and hormesis: human tumor cell lines commonly display hormetic (biphasic) dose responses. Crit. Rev. Toxicol. 35, 463–582. https://doi.org/10.1080/10408440591034502.

Coperchini, F., Awwad, O., Rotondi, M., Santini, F., Imbriani, M., Chiovato, L., 2017. Thyroid disruption by perfluorooctane sulfonate (PFOS) and perfluorooctanoate (PFOA). J. Endocrinol. Invest. 40, 105–121. https://doi.org/10.1007/s40618-016-0572-z.

Coperchini, F., Croce, L., Pignatti, P., Ricci, G., Gangemi, D., Magri, F., Imbriani, M., Rotondi, M., Chiovato, L., 2021. The new generation PFAS C6O4 does not produce adverse effects on thyroid cells in vitro. J. Endocrinol. Invest. 44, 1625–1635. https://doi.org/10.1007/s40618-020-01466-4.

Crowley, L.C., Marfell, B.J., Waterhouse, N.J., 2016. Analyzing cell death by nuclear staining with Hoechst 33342. Cold Spring Harb. Protoc. https://doi.org/10.1101/pdb.prot087205.

DeWitt, J.C., Peden-Adams, M.M., Keller, J.M., Germolec, D.R., 2012. Immunotoxicity of perfluorinated compounds: recent developments. Toxicol. Pathol. 40, 300–311. https://doi.org/10.1177/0192623311428473.

Estandarte, A.K., Botchway, S., Lynch, C., Yusuf, M., Robinson, I., 2016. The use of DAPI fluorescence lifetime imaging for investigating chromatin condensation in human chromosomes. Sci. Rep. 6, 31417. https://doi.org/10.1038/srep31417.

Fair, P.A., Houde, M., 2018. Poly- and perfluoroalkyl substances in marine mammals. Mar. Mammal. Ecotoxicol. Impacts Mult. Stress. Popul. Heal 117–145. https://doi.org/10.1016/B978-0-12-812144-3.00005-X.

Fair, P.A., Adams, J., Mitchum, G., Hulsey, T.C., Reif, J.S., Houde, M., Muir, D., Wirth, E., Wetzel, D., Zolman, E., McFee, W., Bossart, G.D., 2010. Contaminant blubber burdens in Atlantic bottlenose dolphins (Tursiops truncatus) from two southeastern US estuarine areas: Concentrations and patterns of PCBs, pesticides, PBDEs, PFCs, and PAHs. Sci. Total Environ. 408, 1577–1597. https://doi.org/10.1016/j.scitotenv.2009.12.021.

Filippi-Chiela, E.C., Oliveira, M.M., Jurkovski, B., Callegari-Jacques, S.M., da Silva, V.D., Lenz, G., 2012. Nuclear morphometric analysis (NMA): Screening of senescence, apoptosis and nuclear irregularities. PLoS One 7. https://doi.org/10.1371/journal.pone.0042522.

Finos, L., 2018, flip: Multivariate Permutation Tests.R package version 2.5.0. ⟨https://CRAN.R-project.org/package=flip⟩.

Günes-Bayir, A., Kocyigit, A., Guler, E.M., Dadak, A., 2020. In vitro hormetic effect investigation of thymol on human fibroblast and gastric adenocarcinoma cells. Mol. https://doi.org/10.3390/molecules25143270.

Hagenaars, A., Vergauwen, L., De Coen, W., Knapen, D., 2011. Structure–activity relationship assessment of four perfluorinated chemicals using a prolonged zebrafish early life stage test. Chemosphere 82, 764–772. https://doi.org/10.1016/j.chemosphere.2010.10.076.

Hu, W., Jones, P.D., Upham, B.L., Trosko, J.E., Lau, C., Giesy, J.P., 2002. Inhibition of gap junctional intercellular communication by perfluorinated compounds in rat liver and dolphin kidney epithelial cell lines in vitro and Sprague-Dawley rats in vivo. Toxicol. Sci. 68, 429–436. https://doi.org/10.1093/toxsci/68.2.429.

Jabeen, M., Fayyaz, M., Irudayaraj, J., 2020. Epigenetic Modifications, and Alterations in Cell Cycle and Apoptosis Pathway in A549 Lung Carcinoma Cell Line upon Exposure to Perfluoroalkyl Substances. Toxics. https://doi.org/10.3390/toxics8040112.

Lam, J.C.W., Lyu, J., Kwok, K.Y., Lam, P.K.S., 2016. Perfluoroalkyl Substances (PFASs) in Marine Mammals from the South China Sea and Their Temporal Changes 2002-2014: Concern for Alternatives of PFOS? Environ. Sci. Technol. 50, 6728–6736. https://doi.org/10.1021/acs.est.5b06076.

Lau, C., Thibodeaux, J.R., Hanson, R.G., Narotsky, M.G., Rogers, J.M., Lindstrom, A.B., Strynar, M.J., 2006. Effects of Perfluorooctanoic Acid Exposure during Pregnancy in the Mouse. Toxicol. Sci. 90, 510–518. https://doi.org/10.1093/toxsci/kfj105.

Liu, M., Song, S., Hu, C., Tang, L., Lam, J.C.W., Lam, P.K.S., Chen, L., 2020. Dietary administration of probiotic Lactobacillus rhamnosus modulates the neurological toxicities of perfluorobutanesulfonate in zebrafish. Environ. Pollut. 265, 114832 https://doi.org/10.1016/j.envpol.2020.114832.

López-Berenguer, G., Bossi, R., Eulaers, I., Dietz, R., Peñalver, J., Schulz, R., Zubrod, J., Sonne, C., Martínez-López, E., 2020. Stranded cetaceans warn of high perfluoroalkyl substance pollution in the western Mediterranean Sea. Environ. Pollut. 267 https://doi.org/10.1016/j.envpol.2020.115367.

Luebker, D.J., York, R.G., Hansen, K.J., Moore, J.A., Butenhoff, J.L., 2005. Neonatal mortality from in utero exposure to perfluorooctanesulfonate (PFOS) in Sprague–Dawley rats: Dose–response, and biochemical and pharamacokinetic

parameters. Toxicology 215, 149–169. https://doi.org/10.1016/J.TOX.2005.07.019.

Lynch, K.M., Fair, P.A., Houe, M., Muir, D.C.G., Kannan, K., Bossart, G.D., Bartell, S.M., Gribble, M.O., 2019. Temporal Trens in Per- an Polyfluoroalkyl Substances in Bottlenose Dolphins (Tursiops truncatus) of Inian River Lagoon, Floria a Charleston, South Carolina. Environ. Sci. Technol. 53, 14194–14203. https://doi.org/10.1021/acs.est.9b04585.

Mollenhauer, M.A.M., Carter, B.J., Peden-Adams, M.M., Bossart, G.D., Fair, P.A., 2009. Gene expression changes in bottlenose dolphin, Tursiops truncatus, skin cells following exposure to methylmercury (MeHg) or perfluorooctane sulfonate (PFOS). Aquat. Toxicol. 91, 10–18. https://doi.org/10.1016/j.aquatox.2008.09.013.

Montelli, S., Suman, M., Corain, L., Cozzi, B., Peruffo, A., 2017. Sexually Diergic Trophic Effects of Estradiol Exposure on Developing Bovine Cerebellar Granule Cells. Neuroendocrinology 104, 51–71. https://doi.org/10.1159/000444528.

Narita, Masashi, Nūnez, S., Heard, E., Narita, Masako, Lin, A.W., Hearn, S.A., Spector, D. L., Hannon, G.J., Lowe, S.W., 2003. Rb-Mediated Heterochromatin Formation and Silencing of E2F Target Genes during Cellular Senescence. Cell 113, 703–716. https://doi.org/10.1016/S0092-8674(03)00401-X.

Pesarin, F., 2001. Multivariate Permutation Tests: With Applications in Biostatistics, Vol. 240. Wiley, Chichester.

Pierozan, P., Karlsson, O., 2018. PFOS induces proliferation, cell-cycle progression, and malignant phenotype in human breast epithelial cells. Arch. Toxicol. 92, 705–716. https://doi.org/10.1007/s00204-017-2077-8.

R Core Team, 2021. R: A Language and Environment for Statistical Computing. R Foundation for Statistical Computing,, Vienna, Austria (URL). ⟨https://www.R-project.org/⟩.

Reistad, T., Fonnum, F., Mariussen, E., 2013. Perfluoroalkylated compounds induce cell death and formation of reactive oxygen species in cultured cerebellar granule cells. Toxicol. Lett. 218, 56–60. https://doi.org/10.1016/J.TOXLET.2013.01.006.

Roukos, V., Pegoraro, G., Voss, T.C., Misteli, T., 2015. Cell cycle staging of individual cells by fluorescence microscopy. Nat. Protoc. 10, 334–348. https://doi.org/10.1038/nprot.2015.016.

Schorpp, K., Rothenaigner, I., Maier, J., Traenkle, B., Rothbauer, U., Hadian, K., 2016. A multiplexed high-content screening approach using the chromobody technology to identify cell cycle modulators in living cells. J. Biomol. Screen. 21 (9), 965–977. https://doi.org/10.1177/1087057116641935.

Sciancalepore, G., Pietroluongo, G., Centelleghe, C., Milan, M., Bonato, M., Corazzola, G., Mazzariol, S., 2021. Evaluation of per- and poly-fluorinated alkyl substances (PFAS) in livers of bottlenose dolphins (Tursiops truncatus) found stranded along the northern Adriatic Sea. Environ. Pollut. 291, 118186 https://doi.org/10.1016/J.ENVPOL.2021.118186.

Shabalina, I.G., Panaretakis, T., Bergstrand, A., DePierre, J.W., 1999. Effects of the rodent peroxisome proliferator and hepatocarcinogen, perfluorooctanoic acid, on apoptosis in human hepatoma HepG2 cells. Carcinogenesis 20, 2237–2246. https://doi.org/10.1093/carcin/20.12.2237.

Shahsavari, E., Rouch, D., Khudur, L.S., Thomas, D., Aburto-Medina, A., Ball, A.S., 2021. Challenges and Current Status of the Biological Treatment of PFAS-Contaminated Soils. Front. Bioeng. Biotechnol. 8, 1493. https://doi.org/10.3389/fbioe.2020.602040.

Slotkin, T.A., MacKillop, E.A., Meinick, R.L., Thayer, K.A., Seidler, F.J., 2008. Developmental neurotoxicity of perfluorinated chemicals modeled in vitro. Environ. Health Perspect. 116, 716–722. https://doi.org/10.1289/ehp.11253.

Solari, A., Finos, L., Goeman, J.J., 2014. Rotation-based multiple testing in the multivariate linear model. Biometrics 70, 954–961. https://doi.org/10.1111/biom.12238.

Sturm, R., Ahrens, L., 2010. Trends of polyfluoroalkyl compounds in marine biota and in humans. Environ. Chem. 7, 457–484. https://doi.org/10.1071/EN10072.

Suman, M., Giacomello, M., Corain, L., Ballarin, C., Montelli, S., Cozzi, B., Peruffo, A., 2012. Estradiol effects on intracellular Ca2+ homeostasis in bovine brain-derived endothelial cells. Cell Tissue Res 350, 109–118. https://doi.org/10.1007/s00441-012-1460-2.

Sunderland, E.M., Hu, X.C., Dassuncao, C., Tokranov, A.K., Wagner, C.C., Allen, J.G., 2019. A review of the pathways of human exposure to poly- and perfluoroalkyl substances (PFASs) and present understanding of health effects. J. Expo. Sci. Environ. Epidemiol. 29, 131–147. https://doi.org/10.1038/s41370-018-0094-1.

Vakifahmetoglu, H., Olsson, M., Zhivotovsky, B., 2008. Death through a tragedy: Mitotic catastrophe. Cell Death Differ. 15, 1153–1162. https://doi.org/10.1038/cdd.2008.47.

Wen, Y., Mirji, N., Irudayaraj, J., 2020. Epigenetic toxicity of PFOA and GenX in HepG2 cells and their role in lipid metabolism. Toxicol. Vitr. 65, 104797 https://doi.org/10.1016/J.TIV.2020.104797.